Klarman, A., Shaklai, N., & Daniel, E. (1977) *Biochim. Biophys. Acta 490*, 322–330.
Lakowicz, J. R., & Weber, G. (1973) *Biochemistry 12*, 4161–4170.
Lehrer, S. S. (1971) *Biochemistry 10*, 3254–3263.
Linzen, B., Soeter, N. M., Riggs, A. F., Schneider, H. J., Schartau, W., Moore, M. D., Yokota, E., Behrens, P. Q., Nakashima, H., Takagi, T., Nemoto, T., Vereijken, J. M., Bak, H. J., Beintema, J. J., Volbeda, A., Gaykema, W. P. J., & Hol, W. G. J. (1985) *Science (Washington, D.C.) 229*, 519–529.
Ma, J. K. H., Luzzi, L. A., Ma, T. Y. C., & Li, N. C. (1977) *J. Pharm. Sci. 66*, 1684–1687.
Moog, R. S., Kuki, A., Fayer, M. D., & Boxer, S. G. (1984) *Biochemistry 23*, 1564–1571.
Ricchelli, F. (1982) *Med. Biol. Environ, 10*, 327–331.
Ricchelli, F., & Salvato, B. (1979) *Eur. J. Biochem. 94*, 199–205.
Ricchelli, F., & Zatta, P. (1985) *Med. Biol. Environ. 13*, 105–108.
Ricchelli, F., Salvato, B., Filippi, B., & Jori, G. (1980) *Arch. Biochem. Biophys. 202*, 277–288.
Ricchelli, F., Tealdo, E., & Salvato, B. (1983) *Life Chem. Rep., Suppl. Ser. 1*, 301–304.
Ricchelli, F., Jori, G., Tallandini, L., Zatta, P., Beltramini, M., & Salvato, B. (1984) *Arch. Biochem. Biophys. 235*, 461–469.
Ricchelli, F., Filippi, B., Gobbo, S., Simoni, E., Tallandini, L., & Zatta, P. (1986) in *Invertebrate Oxygen Carriers* (Linzen, B., Ed.) pp 235–239, Springer, Berlin.
Salvato, B., & Zatta, P. (1977) in *Structure and Function of Hemocyanin* (Bannister, J. V., Ed.) pp 245–252, Springer, Berlin.
Salvato, B., Ghiretti-Magaldi, A., & Ghiretti, F. (1979) *Biochemistry 18*, 27–37.
Salvato, B., Giacometti, G. M., Alviggi, M., & Giacometti, G. (1986a) in *Invertebrate Oxygen Carriers* (Linzen, B., Ed.) pp 457–462, Springer, Berlin.
Salvato, B., Giacometti, G. M., Alviggi, M., & Giacometti, G. (1986b) in *Invertebrate Oxygen Carriers* (Linzen, B., Ed.) pp 453–456, Springer, Berlin.
Shakali, N., & Daniel, E. (1970) *Biochemistry 9*, 564–568.
Shaklai, N., & Daniel, E. (1972) *Biochemistry 11*, 2199–2203.
Shaklai, N., Gafni, A., & Daniel, E. (1978) *Biochemistry 17*, 4438–4442.
Symons, M. C. R., & Petersen, R. L. (1978) *Biochim. Biophys. Acta 535*, 247–252.
Tamburro, A. M., Salvato, B., & Zatta, P. (1976) *Comp. Biochem. Physiol., B: Comp. Biochem. 55B*, 347–356.
Teale, F. W. J., & Badley, R. A. (1970) *Biochem. J. 116*, 341.
Yen Fager, L., & Alben, J. O. (1972) *Biochemistry 11*, 4786–4792.
Yokota, E., Moore, M. D., Behrens, P. Q., & Riggs, A. F. (1983) *Life Chem. Rep. Suppl. Ser. 1*, 75–80.

Proton NMR Characterization of Isomeric Sulfmyoglobins: Preparation, Interconversion, Reactivity Patterns, and Structural Features†

Mariann J. Chatfield, Gerd N. La Mar,* and Robert J. Kauten
Department of Chemistry, University of California, Davis, California 95616
Received April 1, 1987; Revised Manuscript Received May 20, 1987

ABSTRACT: The preparations of sulfmyoglobin (sulf-Mb) by standard procedures have been found heterogeneous by ^{1}H NMR spectroscopy. Presented here are the results of a comprehensive study of the factors that influence the selection among the three dominant isomeric forms of sperm whale sulf-Mb and their resulting detailed optical and ^{1}H NMR properties as related to their detectability and structural properties of the heme pocket. A single isomer is formed initially in the deoxy state; further treatment in any desired oxidation/ligation state can yield two other major isomers. Acid catalysis and chromatography facilitate formation of a second isomer, particularly in the high-spin state. At neutral pH, a third isomer is formed by a first-order process. The processes that alter oxidation/ligation state are found to be reversible and are judged to affect only the metal center, but the three isomeric sulf-Mbs are found to exhibit significantly different ligand affinity and chemical stability. The present results allow, for the first time, a rational approach for preparing a given isomeric sulf-Mb in an optimally pure state for subsequent characterization by other techniques. While optical spectroscopy can distinguish the alkaline forms, only ^{1}H NMR clearly distinguishes all three ferric isomers. The ring current shifts in the carbonyl complexes of reduced sulf-Mb complexes support saturation for a pyrrole in each isomer. The hyperfine shift patterns in the various oxidation/spin states of sulf-Mbs indicate relatively small structural alteration, and the proximal and distal sides of the heme suggest that peripheral electronic effects are responsible for the differentially reduced ligand affinities for the three isomeric sulf-Mbs. The first ^{1}H NMR spectra of sulfhemoglobins are presented, which indicate a structure similar to that of the initially formed sulf-Mb isomer but also suggest the presence of a similar molecular heterogeneity as found for sulf-Mb, albeit to a smaller extent.

Sulfhemoglobin (sulf-Hb)[1] is a green heme protein that is physiologically inactive (Park & Nagel, 1984). Since its discovery (Hoppe-Seyler, 1866), this modified hemoglobin and an analogous complex of myoglobin, sulf-Mb, have undergone a variety of studies designed to determine the structural al-

† This work was supported by a grant from the National Institutes of Health (GM-26226).
* Author to whom correspondence should be addressed.

[1] Abbreviations: sulf-Hb, sulfhemoglobin; sulf-Mb, sulfmyoglobin; S_AMb, S_BMb, and S_CMb, isomeric forms of sulfmyoglobin; Mb, myoglobin; Hb, hemoglobin.

0006-2960/87/0426-6939$01.50/0

teration giving rise to their unique optical spectra and reduced oxygen affinities (Keilen, 1933; Nichols, 1961; Morell et al., 1967; Berzofsky et al., 1971b). ^{35}S studies on sulf-Mb, a simple model for sulf-Hb, demonstrated that one atom of sulfur is bound to the heme periphery (Berzofsky et al., 1972). The characteristic visible spectrum led to the proposal of a chlorin-like structure where the sulfur is often envisaged as being incorporated as an episulfide across a pyrrole β–β bond (Berzofsky et al., 1972). Various spectroscopic methods have been utilized to characterize sulf-Mb complexes, including optical, ESR, resonance Raman, and NMR spectroscopy (Berzofsky et al., 1971a,b, 1972a,b; Andersson et al., 1984; Timkovich & Vavra, 1985; Chatfield et al., 1986a–c; Magliozzo & Peisach, 1986; Bondoc et al., 1986). The latter method has revealed added complexities in the unraveling of the structure of sulf-Mb (Chatfield et al., 1986a,c), as well as provided the only clear identification of the affected pyrrole (Chatfield et al., 1986b,c; Bondoc et al., 1986).

The complicating discovery was that sulf-Mb is heterogeneous (Chatfield et al., 1986a,c). Several distinct forms have been observed in the sulf-Mb formed by the standard method of preparation (Berzofsky et al., 1971a). The presence of these forms is not related to the presence of heme rotational disorder (La Mar et al., 1983; Chatfield et al., 1986a). Three of the forms, which we have designated S_AMb, S_BMb, and S_CMb in the order of their appearance (Chatfield et al., 1986c), were observed as major products, with their formation depending on sample manipulations (Chatfield et al., 1986a,c). The third derivative, S_CMb, could only be prepared in the presence of a 4-vinyl group on the heme (I), indicating that the pyrrole

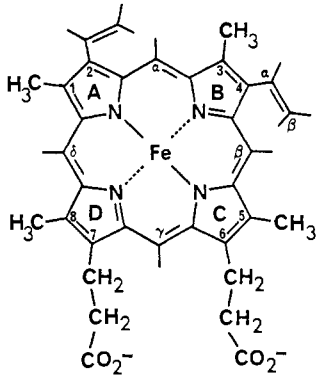

I

ring B and the 4-vinyl group were involved in the formation of this isomer (Chatfield et al., 1986b). In the absence of the 4-vinyl group, yet another two new sulf-Mb derivatives were identified, which were red and possessed optical spectra very similar to, but distinct from, the native protein (Chatfield et al., 1986c).

^2H isotope labeling and spin decoupling of the NMR spectrum of a green pigment extracted from S_CMb identified a saturated pyrrole B with a cyclized thioether, as depicted in IIc (Chatfield et al., 1986b). The ability to reconstitute

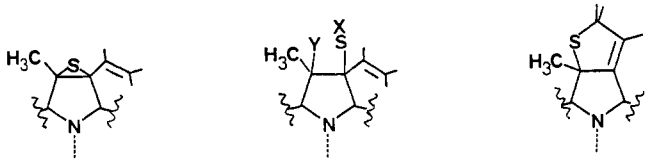

IIa IIb IIc

fresh apo-Mb with this green pigment to regenerate the characteristic ^1H NMR spectra of metS_CMbCN established that the prosthetic group possessed the same reacted 4-vinyl as in IIc (Chatfield et al., 1986b). Chemical derivatization of a similar extracted group yielded the same conclusions (Bondoc et al., 1986). The chemical nature of the other two dominant structures, as well as the reaction pathways for their formation, however, remains unresolved.

It is the purpose of the present paper to delineate the factors that influence the formation of the individual isomeric sulf-Mbs. The number of different species observed by ^1H NMR when sulf-Mb is prepared by standard methods (Berzofsky et al., 1971a) is large (Chatfield et al., 1986c). However, to date, only three different species have been generated as the dominant forms of sulf-Mb, and in this study we restrict outselves to a characterization of the conditions that favor their formation and interconversion.[2] Such characterization of their formation will allow preparation of optimally pure isomeric forms for subsequent structural characterization by other spectroscopic techniques. Moreover, the preparation of sulf-Mbs in a variety of oxidation/ligation states reveals that the isomeric components possess distinct reactivity patterns.

The spectroscopic technique we chose for characterizing sulf-Mb is ^1H NMR, as this method first allowed identification of the various isomers. The ability to detect the three dominant isomeric sulf-Mbs has been demonstrated for their low-spin met-cyano derivatives, which yield the optimal resolution (Chatfield et al., 1986a–c). Some preliminary ^1H NMR spectra of high-spin ferric sulf-Mb complexes have been reported (Timkovich & Vavra, 1985; Chatfield et al., 1986a) and chemical shifts for a single resonance of the reduced carbonyl complex cited (Bondoc et al., 1986). The spectra of the deoxy forms of sulf-Mb have been reported to exhibit only broad and poorly resolved lines (Timkovich & Vavra, 1985). It is our interest, however, to both assess the utility of detecting the isomeric sulf-Mbs in all other attainable oxidation/spin states of the iron and to utilize the inherent diverse information content on heme–protein interaction of the different oxidation/spin states of iron [La Mar, 1979; La Mar & Walker (Jensen), 1979] to probe the potential structural basis for the dramatically altered ligand affinity of sulf-Mbs (Berzofsky et al., 1971b, 1972a).

Lastly, we present the first ^1H NMR spectra of sulf-Hb preparations which indicate that some aspects of the structural heterogeneity characterized for sulf-Mb may be relevant to sulf-Hb.

Materials and Methods

Sperm whale myoglobin was purchased from Sigma Chemical Co. and used without further purification. For CO complexes, labile backbone protons were exchanged by dissolution of the native met-aquo protein into 0.2 M NaCl in ^2H_2O, followed by storage at 22 °C for 30 days. Hemoglobin was obtained from a local blood bank and was isolated and purified in the carbonyl form by standard procedures (Nagai et al., 1979).

Sulf-Mb Preparation. Solutions of ferrous sulf-Mb (approximately 3 mM in 0.1 M potassium phosphate buffer in either H_2O or ^2H_2O) were prepared by standard methods (Berzofsky et al., 1971a). Proteins were converted to a desired

[2] Multiple side products are observable, which are labeled x in the spectra. Most of these products are formed primarily in the equilibration of the low-spin states and never account for more than 10% of the total protein observed. Their formation is largest in the met-cyano state, where it may be minimized by equilibration at 4 °C; such influence of temperature on the formation of minor products has not been observed for any other state.

state in situ: sulf-MbCO was prepared by the addition of excess CO to the deoxy protein at 0 °C, the met-aquo state was prepared by addition of 40 μL of 0.2 M $K_3Fe(CN)_6$ to 1 mL of the ferrous protein, and metsulf-MbCN was formed by the addition of 2 equiv of KCN per heme of the oxidized protein. The pH was adjusted by the addition of aliquots of 1 M potassium phosphate buffer at pH 6 and was determined on a Beckman Model 3550 pH meter equipped with an Ingold microcombination electrode; the values are not corrected for isotope effects. Each sample was then divided and half observed in situ, while the other portion was subjected to chromatography on Sephadex G-25 (1.5 × 36 cm) equilibrated at the same pH, buffer, and ligand strength as in the in situ protein sample. Each chromatographed sample was then concentrated by ultrafiltration (Amicon 8MC, YM5 membrane) and exchanged into 0.1 M phosphate buffer at the same pH and ligand concentration as for the initial preparation. All manipulations were performed at 4 °C, with the in situ portion of each sample being stored at 4 °C during these processes and observed over the same time span as the chromatographed protein. Following initial preparation, the samples were allowed to equilibrate for varying periods of time at 4 or 22 °C.

Sulf-Hb Preparation. Sulf-Hb was prepared from Hb (Carrico et al., 1978a) to give the green product in ~50% yield. Following chromatography of the green ferrous sulf protein on Sephadex G-25, the sample was concentrated to 1 mL. To obtain the spectrum shown in Figure 8B, the deoxy protein was passed through a second column upon which had been layered a 10-fold molar excess of $K_3Fe(CN)_6$. The eluted ferric sulf-Hb was collected and converted to the met-cyano state by the addition of 2 equiv of KCN per heme and concentrated through ultrafiltration (Amicon 8MC, YM10 membrane). The resulting solution of 1.5 mM protein was exchanged into 0.1 M potassium phosphate buffer, pH 8.0 in ^2H_2O, in the presence of a 2-fold excess of KCN. An alternate method of preparation (Figure 8C) involved freezing the chromatographed deoxy protein at 77 K. Upon thawing, $K_3Fe(CN)_6$ was added directly to the protein and removed by ultrafiltration. The sample was then exchanged into ^2H_2O buffer as described above.

Optical Spectra. Optical spectra were observed at ambient temperatures on a Hewlett-Packard 8540A UV–vis spectrophotometer using 1-cm light path quartz cells referenced against water. Sample composition was determined from the peak areas of the corresponding ^1H NMR spectrum, utilizing the line shape fitting program Nicolet NMCCAP. Optical spectra were obtained by diluting 10 μL of 3 mM protein into 2 mL of ^2H_2O in the optical cell.

^1H NMR Spectra. A Nicolet NTC-360 spectrometer was used to obtain 360-MHz ^1H NMR spectra. Typical spectra consisted of 10^3–10^4 transients of 8192 points over an 8–110-kHz bandwidth using a 7-μs 90° pulse. The residual water signal was suppressed by a decoupler pulse. All chemical shifts are given in parts per million from internal 2,2-dimethyl-2-silapentane-5-sulfonate (DSS). NMR difference spectra were generated by using a subroutine of the NMC-1280 program, where spectra are separated by the sequential removal of each individual spectrum of known identity. For example, Figure 7A was obtained by the subtraction of Figure 2F from Figure 2D, canceling B_1 and B_2, followed by subtraction of Figure 2A, nulling peaks M_1 and M_2.

Results

Formation of Isomeric Sulf-Mbs. Previous reports on the formation of the isomeric sulf-Mbs revealed that the factors contributing to the selection of the isomers included chromatography, solution pH, and time (Chatfield et al., 1986a,c). The various factors, however, were applied neither systematically nor in the same oxidation/ligation state of the protein. Since the state of the iron is in itself an important factor in isomeric selectivity (see below), we consider here the influence of solution conditions on isomer formation and interconversion in each oxidation/ligation state. The met-cyano form of the sulf-Mbs serves as the reference for isomer identity and composition (Chatfield et al., 1986a–c), particularly in cases of spectral overlap in the other oxidation/ligation states.

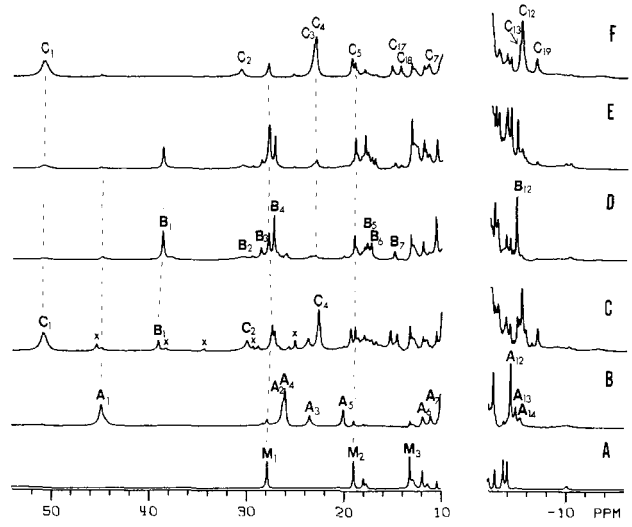

FIGURE 1: 360-MHz ^1H NMR spectra of the met-cyano complexes of the isomeric sulf-Mbs at 20 °C in ^2H_2O. (A) Native metMbCN, pH 7.1. (B) Chromatographed $metS_AMbCN$, pH 7.1; an identical spectrum was observed prior to chromatography. (C) Products of chromatographing $metS_AMbCN$ at pH 6.0 and storing at 4 °C for 2 months; new products $metS_BMbCN$ and $metS_CMbCN$ are observed (see below). Slight nonalignment of the same resonance connected by dotted lines is due to a small pH dependence of shifts below pH 7. Several minor side products[2] are present with resonances labeled x; these resonances resemble, but do not belong to, any of the major species of sulf-MbCN. (D) $MetS_BMbCN$ made by ligating with cyanide the sample of Figure 2F, pH 7.1. (E) Sample from trace D following 7 days at 22 °C (not to same vertical scale as trace D); increased metMbCN[5] is observed. (F) $MetS_CMbCN$ resulting from oxidizing and ligating the sample of Figure 4C, pH 7.1. Peaks of $metS_AMbCN$, $metS_BMbCN$, $metS_CMbCN$, and native metMbCN are labeled A_i, B_i, C_i, and M_i, respectively; impurities[2] are labeled x.

Met-cyano Sulf-Mbs. The hyperfine-shifted portions of the 360-MHz ^1H NMR spectra of sperm whale metMbCN are given in Figure 1A. The prominent heme methyl resonances M_1, M_2, and M_3 identify the native protein (Mayer et al., 1974; La Mar et al., 1983).

Immediate oxidation and cyanide ligation of deoxy-sulf-Mb yield the ^1H NMR spectrum shown in Figure 1B. The relative intensities of the non-Mb resonances are in the ratios 1:1 and 1:3 and are consistent with the presence of only one form of metsulf-MbCN [peaks labeled A_i correspond to the form previously designated $metS_AMbCN$ (Chatfield et al., 1986c)]; methyl resonance A_1 identifies this form. Chromatography of this sample in the pH range 6–8 leaves the spectrum unaltered. Hence in this state, chromatography does not facilitate the formation of other isomers (see below).

Equilibration of the chromatographed protein at pH 6 (2 months, 4 °C)[2] produces the ^1H NMR spectrum shown in Figure 1C. Here two new products have been formed: a small amount of $metS_BMbCN$ [peaks B_i with characteristic methyl peak B_1 (Chatfield et al., 1986c)] and a much larger amount of $metS_CMbCN$ [peaks C_i with characteristic methyl peak C_1 (Chatfield et al., 1986b,c)].[3] Equilibration in the pH range

Table I: ^{1}H NMR Chemical Shifts (ppm) of Isomeric Met-cyano Sulf-Mb Complexes, pH 7.1, 20 °C

i[a]	A_i	B_i	C_i
1 (3)	44.75	38.49	50.69
2 (1)	26.12	30.63	30.59
3 (1)	23.41	28.44	22.99
4 (3)	25.93	27.20	22.95
5 (1)	19.97	17.60	19.24
6 (1)	11.83	17.16	*b*
7 (1)	11.01	14.74	11.40
12 (3)	−4.35	−4.74	−5.21
13 (1)	−4.88	*b*	−5.18
14 (1)	−5.35	*b*	*b*
17 (1)			15.11
18 (1)			14.23
19 (1)			−6.74

[a] Peaks labeled as in Figure 1. The number of protons for the resonance is given in parentheses. [b] Not observable with current sample purity.

7–9 also produces $metS_CMbCN$, with negligible formation of $metS_BMbCN$. The product $metS_CMbCN$ is stable for years at 4 °C and alkaline pH; it yields no further isomeric met-cyano sulf-Mb complexes and regenerates only 5% metMbCN per year.

A sample containing predominantly S_BMb can only be prepared in the met-aquo form of the protein (see below). The ^{1}H NMR trace for $metS_BMbCN$ resulting from addition of cyanide to such a sample is illustrated in Figure 1D. Equilibration of this sample for 1 week at 22 °C[4] gives the ^{1}H NMR spectrum of Figure 1E.[5] The chemical shifts of the resolved resonances of the met-cyano isomers are summarized in Table I. Note that $metS_CMbCN$ exhibits three unique peaks (C_{17}, C_{18}, and C_{19}) that have been assigned to the 4-vinyl H_βs and H_α, respectively (Chatfield et al., 1986b).

Met-aquo Sulf-Mb. The 360-MHz ^{1}H NMR spectrum of $metMbH_2O$ is shown in Figure 2A, with prominent heme methyl resonances M_1, M_2, M_3, and M_4 (La Mar et al., 1980).

Oxidation and pH adjustment[6] of freshly prepared deoxy-sulf-Mb provide the ^{1}H NMR spectrum shown in Figure 2B. Here again the relative intensities of the non-Mb peaks are consistent with the presence of only one sulf-Mb isomer, designated $metS_AMbH_2O$ [peaks labeled A_i, marked by A_1 and A_2 (Chatfield et al., 1986a)]. Chromatography of the $metS_AMbH_2O$ sample at pH 7 provides the spectrum shown in Figure 2C. Here ~5% of a second form, designated $metS_BMgH_2O$, is observed, with prominent resonance B_1 at 110 ppm (Chatfield et al., 1986a). Chromatography of $metS_AMbH_2O$ at pH 6 enhances formation of this product as shown in Figure 2D (resonances labeled B_i).

Equilibration of the chromatographed met-aquo protein at pH 7 and 22 °C[4] yields the spectrum shown in Figure 2E. Here increased formation of $metS_BMbH_2O$ is evident, with negligible reversion to $metMbH_2O$ occurring over 8 h. In addition to the resonances corresponding to $metS_BMbH_2O$, several minor changes in the spectrum are observable. These include the appearance of a shoulder to peaks M_1/B_1, a small peak at 48 ppm, a slight asymmetry to A_1, and small changes in the ratios of various peak heights. Conversion to the met-cyano state reveals that approximately 10% $metS_CMbCN$ has formed in addition to the expected $metS_AMbCN$, $metS_BMbCN$, and metMbCN (not shown). Formation of $metS_CMbH_2O$ by a different route (Figure 2G) confirms that

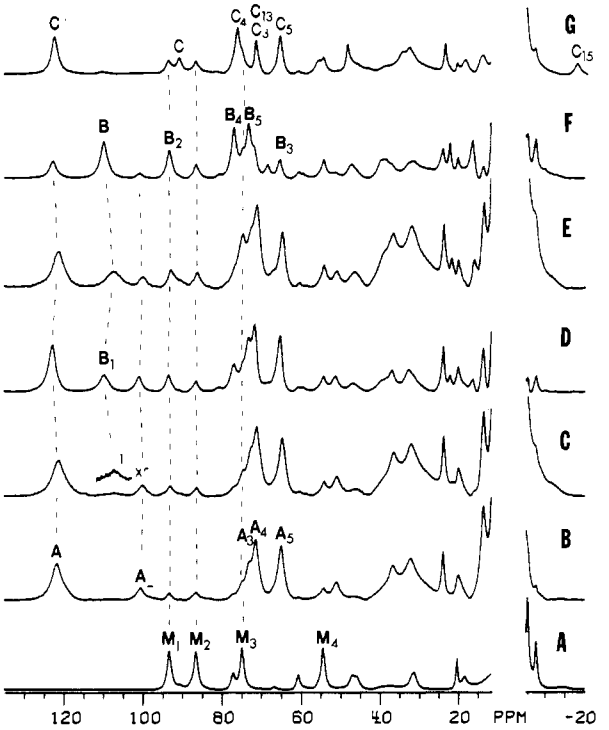

FIGURE 2: 360-MHz ^{1}H NMR spectra of the met-aquo complexes of isomeric sulf-Mb at 20 °C in ^2H_2O. (A) Native $metMbH_2O$, pH 6.0. (B) $MetS_AMbH_2O$ immediately after preparation, oxidation, and pH adjustment to 7.1. (C) Sample from trace B following chromatography at pH 7.1. Peak B_1, corresponding to 5% $metS_BMbH_2O$, is shown in the expanded region. (D) Sample from trace B following chromatography at pH 6.0. The chemical shifts are slightly pH dependent and do not align with the pH 7 traces. (E) Sample from trace C after 8 h at 22 °C, pH 7.0. A shoulder to M_1/B_1, a small peak at 48 ppm, the asymmetry of A_1, and small changes in the ratios of A_i peaks are due to the presence of 10% $metS_CMbH_2O$ (see trace G). (F) Sample of trace D after 8 h at 22 °C, pH 6.0. Note the dramatic increase of B_1 of $metS_BMbH_2O$; a met-cyano trap of this sample is shown in Figure 1D. (G) Sample of Figure 4C following oxidation and pH adjustment to 6.0 to yield primarily $metS_CMbH_2O$. Peaks of $metS_AMbH_2O$, $metS_BMbH_2O$, $metS_CMbH_2O$, and $metMbH_2O$ are labeled A_i, B_i, C_i, and M_i, respectively.

Table II: ^{1}H NMR Chemical Shifts (ppm) of Isomeric Met-aquo Sulf-Mb Complexes, pH 6.0, 20 °C

i[a]	A_i[b]	B_i	C_i[b]
1 (3)	122.80 (−4.4)	109.80	122.29 (0.9)
2 (1)	100.93 (−26)	92.97	90.59 (−26)
3 (1)	73.18 (6.3)	68.28	71.13 (6.1)
4 (3)	71.61 (4.1)	76.04	75.81 (6.8)
5 (3)	65.20 (8.8)	73.06	65.05 (4.1)
6 (1)	51.19 (11)	47.37	55.47 (20)
7 (1)	36.74 (8.9)	39.66	32.43 (7.7)
8 (1)	32.71 (29)	38.46	33.93 (34)
9 (1)	23.75 (−9.3)	22.05	23.07 (−14)
12 (1)		−7.44	
13 (1)			71.13 (−4.4)
14 (1)			47.93 (−0.5)
15 (1)			−18.45 (6.4)

[a] Peaks labeled as in Figure 7. The number of protons in the resonance is given in parentheses. [b] Variable temperature Curie intercepts are given in parentheses.

[3] Other workers have presented evidence of a "high-temperature form" in equine sulf-Mb, with several resonances similar to those of $metS_CMbCN$ (Timkovich & Vavra, 1985).

[4] Equilibration at 4 and 22 °C gives identical products.

[5] In the regeneration process disordered metMbCN (La Mar et al., 1983) is formed as a major product; however, the sum of the area of the combined low-field methyl resonances of each of these two forms of Mb plus that of B_1 remains constant between parts D and E of Figure 1.

[6] At pH >7, an acid–alkaline transition occurs (Berzofsky et al., 1971a), to give a set of resonances that are neither well resolved nor well-defined.

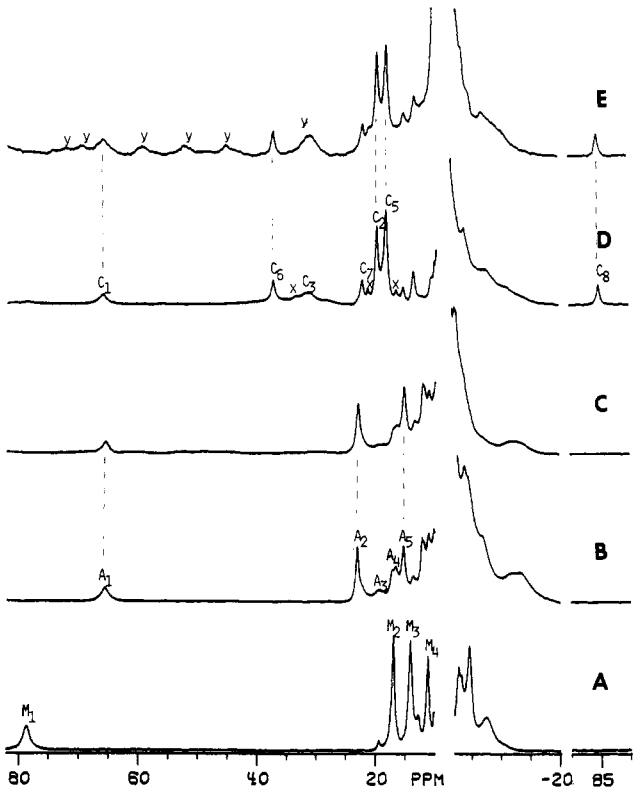

FIGURE 3: 360-MHz ^1H NMR spectra of the deoxy complexes of isomeric sulf-Mbs, pH 8.0, in 90% H_2O/10% ^2H_2O, 20 °C. (A) Native deoxy-Mb. (B) Deoxy-S_AMb immediately after preparation. (C) Deoxy-S_AMb from trace B following chromatography at pH 8.0. S_BMb is present (5%) but is not observed among the deoxy-S_AMb peaks; autoxidation products give rise to the uneven base line. (D) Deoxy-S_CMb formed from metS_CMbCN by the anaerobic addition of 2.5 equiv of sodium dithionite. (E) Sample of Figure 4C following irradiation with light for 15 min under an atmosphere of nitrogen to yield deoxy-S_CMb, as clearly identified by peaks C_6, C_7, and C_8; y identifies the resonances of side products due to photolysis of S_CMbCO. Peaks for deoxy-S_AMb, deoxy-S_CMb, and native Mb are labeled A_i, C_i, and M_i, respectively; x labels minor products. Peaks A_1, C_1, and M_1 are missing in ^2H_2O and arise from the axial His-F8 ring NH (La Mar et al., 1977).

minor changes in the met-aquo spectrum in Figure 2E arise from metS_CMbH$_2$O, the presence of which is difficult to detect beneath numerous coincident metS_AMbH$_2$O resonances. Chemical shifts for each isomer are determined below and are summarized in Table II. Identical products are formed in situ; however, the rate of equilibration is somewhat slower (not shown).

Equilibration of the chromatographed metS_AMbH$_2$O at pH 6.0 for 8 h at 22 °C[4] produces a sample consisting mainly of metS_BMbH$_2$O as shown in Figure 2F. Treatment with CN^- reveals S_BMb to be the major product (Figure 1D), with only 3% S_CMb being formed under these conditions. Further equilibration of the sample produces only native Mb.

Deoxy-sulf-Mb. Figure 3A shows the 360-MHz ^1H NMR spectrum of native deoxy-Mb. Here the resolved heme resonances, M_2–M_4, occur in a highly compressed window of 10–20 ppm (La Mar et al., 1978), while the axial histidine labile ring proton, M_1, resonates downfield at 78 ppm (La Mar et al., 1977).

Studies of this state of sulf-Mb are complicated by the instability of the protein, with autoxidation reported to occur with a half-life at pH 8.0 of 4–6 h at 25 °C (Berzofsky et al., 1971b). The rate of autoxidation may be decreased by removal of dioxygen from the sample; however, the rates of formation of Mb and equilibration products remain unaltered by this procedure (not shown). The hyperfine-shifted portion of the

Table III: ^1H NMR Chemical Shifts (ppm) of Isomeric Deoxy-sulf-Mb Complexes, pH 8.0, 20 °C

i[a]	A_i	C_i
1 (1)	65.54	65.98
2 (3)	22.41	19.97
3 (1)	19.41	31.64
4 (1)	16.51	*b*
5 (3)	15.18	18.43
6 (1)		37.36
7 (1)		22.41
8 (1)		−84.98

[a] Peaks labeled as in Figure 3. The number of protons in the peak is given in parentheses. [b] Not resolved.

^1H NMR spectrum of in situ deoxy-sulf-Mb in the presence of air is illustrated in Figure 3B; a well-resolved spectrum, with similarities to the native deoxy-Mb, is observed. Unreacted deoxy-Mb is not observed, since it is present as the diamagnetic MbO_2 under these conditions (Berzofsky et al., 1971a). The low-field peak A_1 is missing in ^2H_2O and thus is assigned to the His-F8 ring NH. The remaining resolved or partially resolved resonances exhibit intensities for single protons or methyls and hence reflect a single species, deoxy-S_AMb. Oxidation with $Fe(CN)_6^{3-}$ yields the metS_AMbH$_2$O trace (Figure 2B), and ligation by cyanide yields the metS_AMbCN spectrum (Figure 1B). Chromatography of deoxy-S_AMb at pH 8 produces a sample with a ^1H NMR spectrum as shown in Figure 3C; identical results are obtained at pH 7. Conversion to the met-cyano state shows ~5% metS_BMbCN to be present; however, no discernible differences in the deoxy spectrum are observed among the deoxy-S_AMb resonances. At pH 6, more extensive conversion to S_BMb occurs, but the process is not reproducible, and rapid autoxidation obscures the results. However, a trap of a sample that has not autoxidized extensively shows significant S_BMb to be present (not shown), indicating that formation of S_BMb does occur at acidic pH in the deoxy state.

Equilibration of deoxy-S_AMb at pH 6–8 and 22 °C[4] for periods of up to 3 days yields a spectrum (not shown) that shows increased formation of the met-aquo derivatives of all species, but with no indication of the presence of deoxy-S_CMb (see below). Thus, the rates of interconversion of these isomeric sulf-Mbs in the deoxy state are generally not competitive with autoxidation. Essentially pure deoxy-S_CMb, produced by anaerobic dithionite reduction of metS_CMbCN (see below), yields the ^1H NMR spectrum in Figure 3D. The single proton peak C_1 is missing in ^2H_2O solution and hence can be assigned to the axial His ring NH. The chemical shifts for isomeric deoxy-sulf-Mbs are summarized in Table III. Note the unprecedented upfield-shifted single proton peak C_8 and the additional single proton low-field signals C_6 and C_7 in deoxy-S_CMb that are not detected in deoxy-S_AMb.

Carbonmonoxy-sulf-Mb. MbCO is diamagnetic, with resolved resonances of Figure 4A involving the methyls of amino acids Val-E11 (M_{10}) and Leu-B10 (M_9) upfield, and the hemin meso protons (M_1–M_4) occurring in the downfield region (Shulman et al., 1970; Bradbury et al., 1982; Mabbutt & Wright, 1985).

Chromatography of carbonmonoxy-sulf-Mb produces a sample with ^1H NMR spectrum shown in Figure 4B. An identical spectrum is observed in situ. Examination of the spectrum reveals methyl resonance A_{10} of S_AMbCO at −2 ppm, just downfield of the methyl group M_{10} of the unreacted protein, as previously cited (Bondoc et al., 1986). Several single-proton resonances distinct from MbCO are also observed at low fields (A_1–A_3 in Figure 4B), which can be attributed to meso Hs (Scheer & Katz, 1975).

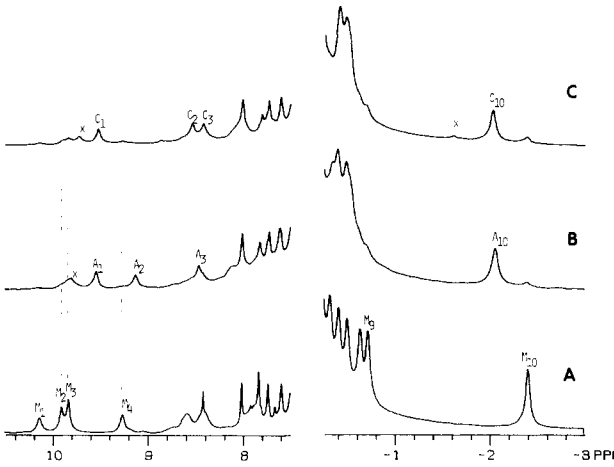

FIGURE 4: 360-MHz ^1H NMR spectra of the diamagnetic carbonyl complexes of isomeric sulf-Mb, pH 8.0 in ^2H_2O, 20 °C. (A) Native MbCO. (B) S_AMbCO after chromatography at pH 8.0; a sample that was not chromatographed gave an identical spectrum. (C) S_CMbCO prepared upon equilibration of the sample from trace B for 3 days at 22 °C. Peaks for S_AMbCO, S_CMbCO, and native MbCO are labeled A_i, C_i, and M_i, respectively, with x identifying side products.[2] M_9 and M_{10} have been identified as the CH_3 of Leu-B10 and Val-E11, respectively (Shulman et al., 1970).

Table IV: ^1H NMR Chemical Shifts (ppm) of Isomeric Carbonyl-sulf-Mb Complexes, pH 8.0, 20 °C

i^a	A_i	C_i
1 (1)	9.53	9.52
2 (1)	9.12	8.53
3 (1)	8.46	8.41
10 (3)	−2.06	−2.04

[a] Peaks labeled as in Figure 4. The number of protons in the peak is given in parentheses.

Equilibration of S_AMbCO at pH 8 and 22 °C[4] for 3 days gives a sample with a ^1H NMR spectrum as shown in Figure 4C. Although the upfield methyl resonance C_{10} of S_CMbCO remains coincident with A_{10} of S_AMbCO, several unique single-proton resonances consistent with meso Hs are observed in the low-field region of the spectrum, labeled C_1–C_3, and are assigned to arise from S_CMbCO on the basis of the metS_CMbCN produced from this sample (Figure 1F). Regeneration (5–15%) of MbCO occurs during the equilibration process. At pH 6, <5% S_BMbCO is also formed, as detected in the met-cyano trap (not shown); however, no spectral characteristics could be assigned to S_BMbCO distinct from those of S_AMbCO or S_CMbCO. The chemical shifts of the CO-ligated isomeric sulf-Mbs are given in Table IV.

Interconversion of Oxidation/Ligation States. The interconversion of oxidation/ligation states of the isomeric sulf-Mbs is produced by reagents that could, in principle, participate in altering the peripheral functionality. The agents used to make these transformations (Scheme I) are known to affect solely the oxidation/ligation state of the iron in the native heme proteins (Antonini & Brunori, 1971). We find here that the facility of several of these transformations differs appreciably for the isomeric sulf-Mbs.

Ligation of Reduced Sulf-Mbs. The deoxy forms of S_AMb and S_CMb react with carbon monoxide to form S_AMbCO and S_CMbCO. Flushing S_AMbCO with N_2 for 10 min produces deoxy S_AMb, while flushing either S_CMbCO or MbCO has no immediate effect upon these proteins. Vaccum degassing S_CMbCO for 30 min produces deoxy-S_CMb, while also having little effect on MbCO. UV irradiation of S_CMbCO yields deoxy-S_CMb, as shown in Figure 3E. Several broad resonances of other unidentified products (designated y) distinct from

Scheme I

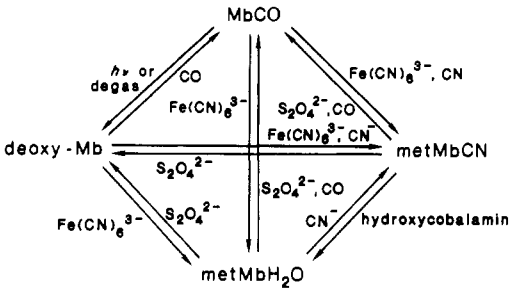

metS_CMbH$_2$O are also observed in the spectrum; however, conversion to the met-cyano protein reveals no evidence for additional forms of sulf-Mb. Similar UV irradiation of S_AMbCO yields solely MbCO, as reported previously (Berzofsky et al., 1972a).

Oxidation/Reduction of Sulf-Mbs. Oxidation with ferricyanide of the deoxy or carbonmonoxy ferrous proteins of S_AMb, S_BMb, and S_CMb generates the corresponding high-spin ferric state of each form, with characteristic resonances shown in parts B, F, and G of Figure 2. Identical sets of resonances are observed when the deoxy proteins are allowed to autoxidize.

Anaerobic reduction of ferric S_AMb and S_BMb proteins with dithionite solution affords solely deoxy-Mb. However, we find that deoxy-S_AMb and deoxy-S_BMb are unstable in the presence of dithionite, yielding native deoxy-Mb within seconds, and thus the inability to detect reduction of the ferric complexes is not surprising. Anaerobic addition of dithionite to metS_CMbCN (or metS_CMbH$_2$O) instantly produces a bright green protein, with the distinctive ^1H NMR spectrum of deoxy-S_CMb shown in Figure 3D. Conversion of the sample back to the met-cyano state produces a compound with a ^1H NMR spectrum identical with that of the starting metS_CMbCN. Deoxy-S_CMb also reacts with dithionite to yield deoxy-Mb, with a half-life of 12 h at 22 °C in the presence of 5 equiv of dithionite, as determined optically. The effect of milder reducing agents such as Fe(EDTA)$^{2-}$ (Lim & Mauk, 1985) is currently being studied.

Ligation of the Oxidized Sulf-Mbs. The met-aquo form of each isomer reacts with cyanide to produce a characteristic low-spin ^1H NMR spectrum (indistinguishable from parts B, D, and F of Figure 1). Upon exposure of the met-cyano isomers to hydroxycobalamin[7] (de Ropp et al., 1985), the met-aquo form of each isomer is slowly produced, as shown for metS_CMbCN in Figure 5. Similar results are obtained for the other isomers (not shown).

Spectral Properties of Individual Isomeric Sulf-Mbs. Using the highly pure samples prepared above, the characteristic optical spectrum of each oxidation/ligation state and ^1H NMR spectrum of the met-aquo state of each isomeric sulf-Mb are presented here. The optical spectra of the deoxy-sulf-Mbs and deoxy-Mb are shown in Figure 6A. No distinct optical bands were observed when the deoxy-S_AMb sample contained up to 30% S_BMb. The electronic absorbances of S_AMbCO, S_CMbCO, and MbCO are shown in Figure 6B. A decrease in intensity and broadening was observed for the S_CMbCO bands as previously reported (Bondoc et al., 1986); however, addition of fresh CO to the cell sharpened the absorbances

[7] Hydroxycobalamin is a vitamin B derivative that exhibits a considerably higher affinity for cyanide than most heme proteins such as myoglobin (Pratt, 1982) and, hence, can qualitatively "strip" cyanide off of met-cyano heme proteins (de Ropp et al., 1985). We thank M. F. Perutz for the valuable suggestion for use of this reagent.

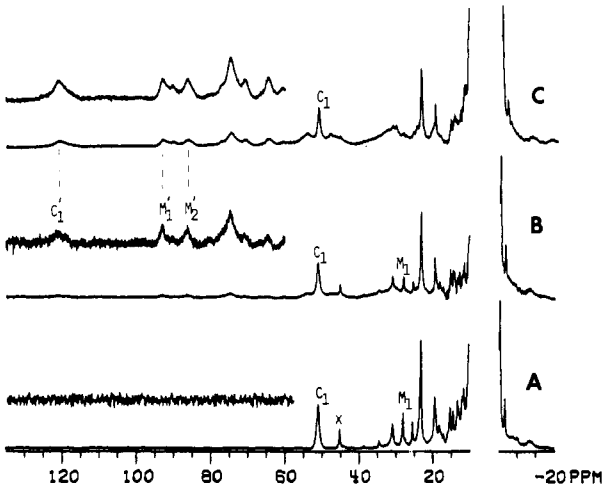

FIGURE 5: 360-MHz ^{1}H NMR spectra of the reaction of metS_CMbCN with hydroxycobalamin,[7] pH 7.1, 20 °C, in ^2H_2O. (A) MetS_CMbCN prepared from equilibration of the sample shown in Figure 1B for 7 days at 22 °C; the sample composition is 75:25 metS_CMbCN:metMbCN. (B) Sample from trace A following the addition of 10 equiv of hydroxycobalamin. Note that comparable amounts of metS_CMbH_2O (C_1') and metMbH_2O (M_1' and M_2') are present; the remainig met-cyano products are 83:17 S_CMb:Mb. (C) Sample from trace C after reaction for 1 h at 22 °C; the residual low-spin met-cyano products are ≥95% metS_CMbCN. Peaks for metS_CMbCN and metMbCN are labeled C_i and M_i, respectively; metS_CMbH_2O and metMbH_2O are labeled C_i' and M_i', respectively. Impurities[2] are labeled x.

Table V: Positions of the Electronic Absorption Maxima of Isomeric Sulf-Mb Complexes

oxidation/ligation state	S_AMb	S_BMb	S_CMb	native Mb
deoxy	618[a]	618[b]	636	556
	420	420[b]	416	434
carbonmonoxy	612	612[b]	626	580
				542
	412[c]	412[b,c]	412[c]	422
met-aquo	718	720	736	634
	594	598	600	504
	408	408	406	408
met-cyano	594	594	596	540
	412	412	412	422

[a] Values to ±1 nm. [b] Only observed to 30% S_BMb in the presence of S_AMb and Mb. [c] Shoulder to Soret of MbCO.

of each CO protein to yield the same scale. Samples containing up to 10% S_BMbCO could not be distinguished optically from S_AMbCO. The optical spectra of metMbH_2O, metS_AMbH_2O, metS_BMgH_2O, and metS_CMbH_2O are displayed in Figure 6C; the 5% metS_BMbH_2O impurity in metS_AMbH_2O did not affect the spectrum. Optical spectra of the met-cyano complexes are shown in Figure 6D; spectra have been previously reported for metS_AMbCN and metS_CMbCN (Chatfield et al., 1986c). The positions of the optical maxima for each state are given in Table V.

In the met-aquo state, the apparent ^{1}H NMR heme methyl resonances overlap extensively. However, resonances corresponding to an individual met-aquo sulf-Mb isomer are obtainable by means of a computer-generated difference spectrum, as described under Materials and Methods. The resulting spectra for the "pure" species are shown in Figure 7. Each isomeric met-aquo sulf-Mb is found to have a distinct set of resonances downfield of 20 ppm, consisting of three methyls, labeled with subscripts 1, 4, and 5, and numerous single-proton resonances. (The large peak at 70 ppm in Figure 7C separates into two single-proton resonances, peaks C_3 and C_{13}, at 40 °C.) Variable temperature data in the form of a Curie plot yield straight lines for each isomer, with apparent intercepts at $T^{-1} = 0$ for metS_AMbH_2O and metS_CH$_2$O listed in Table II. Peaks that appear to be isostructural based on area, chemical shift, and Curie intercept are assigned the same number; chemical shifts are listed in Table II. Note that metS_CMbH_2O exhibits an unusually upfield-shifted single-proton peak, C_{15}, and two more downfield-shifted narrow single-proton peaks, C_{13} and C_{14}, than the other isomers.

Sulfhemoglobin. The hyperfine-shifted portion of the 360-MHz ^{1}H NMR spectrum of met-cyano sulf-Hb is illustrated in part B of Figure 8. The spectrum of native metHbCN is included in Figure 8A for comparison. The residual methyl peaks for unreacted subunits, labeled N_α and N_β, (Ogawa et al., 1972) are readily detected in Figure 8B, but the dominant features are new intense peaks a, b, g, h, j, and k, as well as the small peaks c, d, e, f, and i. A given sample changed little with time, although a variety of preparations yielded slightly different spectra (e.g., see Figure 8C). However, peaks a, e, f, h, and k always maintained the relative ratio 3:1:1:3:3; the set of peaks b, g, i, and j kept the ratio 3:3:1:3, while the ratio of c to d as well as the ratio of either c or d to the other two sets of peaks varied. Attempts to allow a sample to equilibrate as met-aquo sulf-Hb prior to addition of CN^- resulted in the loss of intensity for the set of peaks b, g, i, and j (not shown). Equilibration of a sample of met-cyano sulf-Hb did not change the relative intensities of the non-metHbCN peaks, although regeneration of native Hb did occur. No resonances at lower field than peak a were detected under any condition.

We tentatively attribute the set of peaks a, e, f, h, and k to one subunit of met-cyano sulf-Hb (with a, h, and k as methyls) and peaks b, g, i, and j to the other subunit (b, g, and j as methyls); a second single-proton peak belonging to this set is likely under the g, h, and native metHbCN N_α and N_β composite at 21 ppm. Peaks c and d have less than one proton intensity when compared to either set of resonances and hence do not arise from the same species that result in the set of peaks a, e, f, h, and k, or b, g, i, and j. Thus, the sulf-Hb preparations appear to be heterogeneous.

Discussion

Interconversion of Sulf-Mb. S_AMb is formed exclusively upon reaction of Mb; this product then serves as an intermediate for formation of all other products. The formation of S_BMb depends on both the protein state and the solution conditions. It is facilitated by chromatography in all states, is enhanced at low pH, indicative of acid catalysis, and can be suppressed but not eliminated at alkaline pH. Formation of this isomer is favored in the high-spin states. In general, the rates of S_BMb formation are determined as met-aquo >> deoxy > met-cyano > carbonmonoxy.

At alkaline pH, equilibration of S_AMb yields predominately S_CMb in all oxidation/ligation states except deoxy-S_CMb, where formation is not competitive with autoxidation. The rate of formation of S_CMb is independent of pH as determined by equilibration of metS_AMbCN at 4 °C in the pH range 6–8. Hence the formation of S_CMb proceeds via a first-order process. The overall purity of the S_CMb samples depends upon limiting the formation of S_BMb (see above) and limiting the regeneration of Mb. Formation of S_CMb is fastest and most selective in the CO state, followed by the met-cyano state;[2] rapid formation of metS_BMbH_2O precludes direct formation of predominantly metS_CMbH_2O. Subsequent equilibration of S_CMb in any oxidation/ligation state yields solely the corresponding derivative of the native protein; hence, S_CMb is the terminal sulf-Mb product.

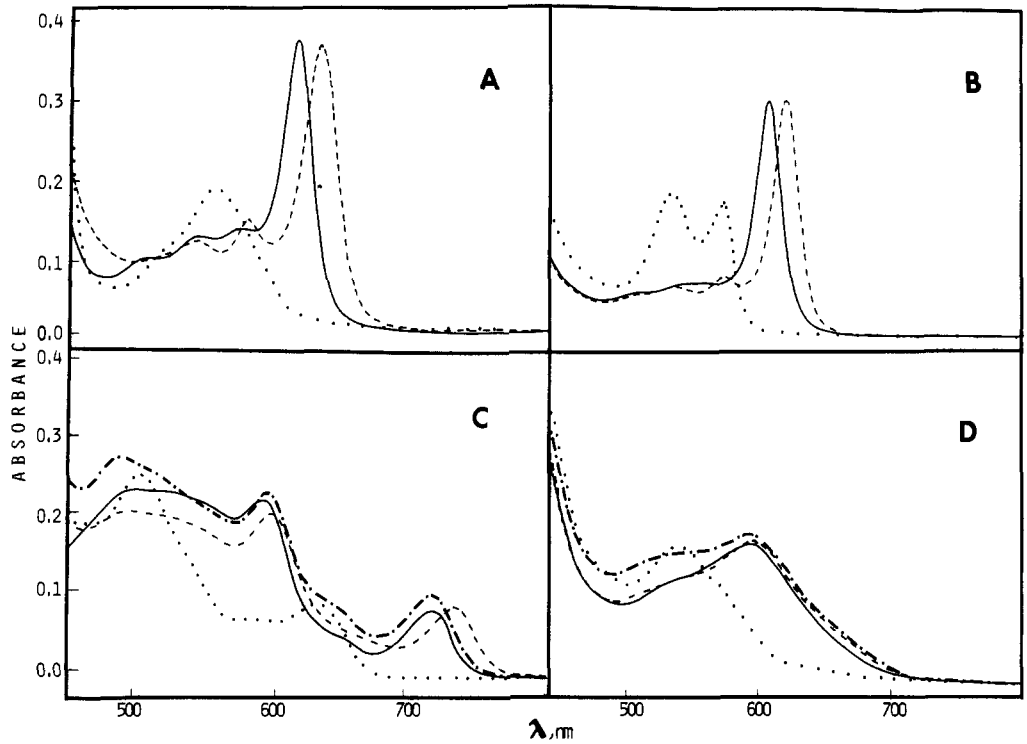

FIGURE 6: Optical spectra of sulf-Mbs. (A) Deoxy-sulf-Mb complexes, pH 8.0: 87% deoxy-S_AMb, 5% S_BMb, 8% MbO_2 (—); 75% deoxy-S_CMb, 15% MbO_2, 10% other (---); deoxy-Mb (···). Deoxy-S_BMb has been prepared to only 30% in the presence of deoxy-S_AMb and has not been detected by optical spectroscopy. ^{1}H NMR spectra of these samples are shown in parts C, D, and A of Figure 3, respectively. (B) Carbonmonoxy-sulf-Mb isomers, pH 8.0: 90% S_AMbCO, 10% MbCO (—); 80% S_CMbCO, 15% MbCO, 5% other (---); MbCO (···). S_BMbCO has only been prepared to <10% in the presence of S_AMbCO or S_CMbCO and is not detectable by optical spectroscopy. ^{1}H NMR spectra are given in parts B, C, and A of Figure 4. The optical spectrum of S_CMbCO prepared following reduction and CO ligation of metS_CMbCN is identical with that shown here. (C) Met-aquo sulf-Mb isomers, pH 6.0: 85% metS_AMbH_2O, 5% metS_BMbH_2O, 10% metMbH_2O (—); 20% metS_AMbH_2O, 62% metS_BMbH_2O, 3% metS_CMbH_2O, 15% metMbH_2O (-·-); 80% metS_CMbH_2O, 15% metMbH_2O, 5% other (---); metMbH_2O (···). The corresponding ^{1}H NMR spectra are shown in parts C, F, G. and A of Figure 2. The 5% metS_BMbH_2O present in the metS_AMbH_2O sample does not affect the spectrum. (D) Met-cyano sulf-Mb complexes, pH 7.1: 90% metS_AMbCN, 10% metMbCN (—); 20% metS_AMbCN, 62% metS_BMbCN, 3% metS_CMbCN, 15% metMbCN (-·-); 80% metS_CMbCN, 15% metMbCN, 5% other (---); metMbCN (···). Corresponding ^{1}H NMR spectra are displayed in parts B, D, F, and A of Figure 1. The percentages were determined by applying a computer fit of the ^{1}H NMR data provided in the met-cyano trap of each sample, as described under Materials and Methods.

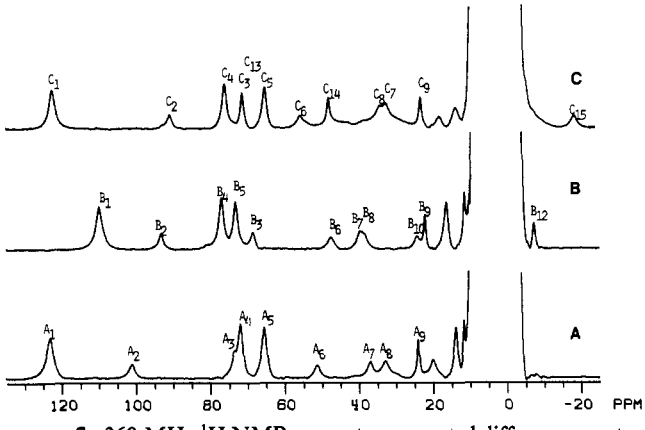

FIGURE 7: 360-MHz ^{1}H NMR computer-generated difference spectra of the individual isomeric met-aquo sulf-Mb complexes, pH 6.0, 20 °C, as described under Materials and Methods. (A) MetS_AMbH_2O with peaks A_i. (B) MetS_BMbH_2O with peaks B_i. (C) MetS_CMbH_2O with peaks C_i; the peak at 70 ppm separates into two single-proton resonances at 40 °C. The broad meso resonances in the region 20–50 ppm are partially lost in the generation of the spectra and are not labeled. Peak numbering was maintained among the isomeric sulf-Mbs to identically label likely isostructural peaks (see text).

Since S_BMb is present in small amounts in every sulf-Mb preparation, the question arises whether this is an intermediate in the conversion of S_AMb to S_CMb or is a terminal side product. That S_BMb is only a terminal side product is demonstrated by equilibrating a predominantly metS_BMbCN sample (Figure 1D) obtained by ligating a metS_BMbH_2O sample (Figure 2F) with CN^-. Equilibration of the sample whose spectrum is shown in Figure 1D yields the trace shown in Figure 1E. Throughout this equilibration, the sum of the areas of A_1 of S_AMb and C_1 of S_CMb remains constant, as does the sum of the area of B_1 of metS_BMbCN and the low-field methyls at 28 ppm of metMbCN;[5] the rate of loss of peaks C_i is the same as in the absence of S_BMb. Thus S_BMb does not generate S_CMb. The established interconversions are summarized in Scheme II.

Scheme II

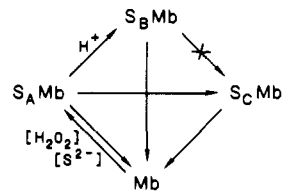

Interconversion of Oxidation/Ligation States. Because of the strong dependence of isomerization on the solution conditions (see above), the potential direct involvement of the reagents in the modification of the chemical functionality must be assessed. To establish that the reagents affect solely the metal center, two criteria are set: the effect of the reagent must be either reversible by standard methods (Scheme I) or attainable by two chemically distinct routes.

Ligation of the reduced proteins is reversible by degassing. Ligation of deoxy-S_CMb is also reversible by photolysis, with transient photoproducts also present. S_AMbCO is not stable

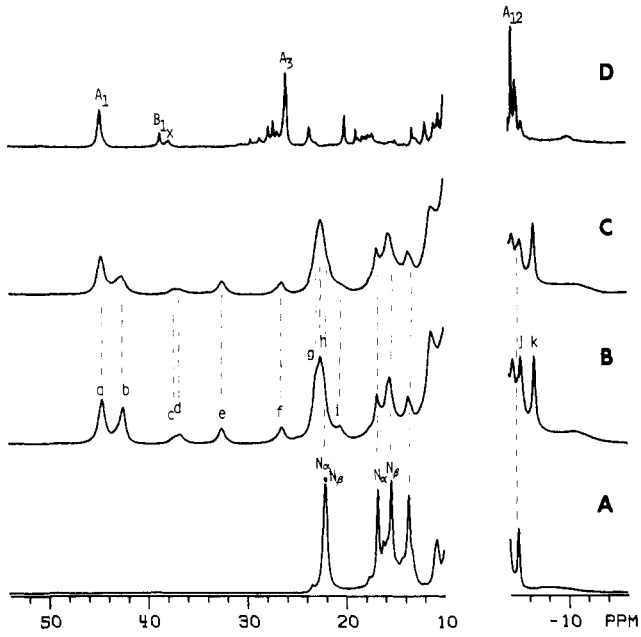

FIGURE 8: 360-MHz ^1H NMR spectra of met-cyano complexes of sulf-Hb and sulf-Mb, pH 8.0, 20 °C, in ^2H_2O. (A) Native metHbCN. (B) Met-cyano sulf-Hb immediately after preparation, chromatography, oxidation on Sephadex G-25 layered with potassium ferricyanide, and ligation with cyanide. (C) Met-cyano sulf-Hb following storage of the chromatographed deoxy protein at 77 K for 1 week, in situ oxidation with potassium ferricyanide, subsequent removal of this reagent by ultrafiltration, and ligation with cyanide. (D) Sample of 80% metS_AMbCN (peaks A_1 and A_{12}) and 20% metS_BMbCN (peaks B_1 and B_{12}). Resonances from native Hb are labeled N_α and N_β, corresponding to the methyl resonances of the α and β subunits, respectively (Ogawa et al., 1972). Sulf-Hb resonances are labeled alphabetically from left to right. Met-cyano sulf-Mb is labeled as in Figure 1.

to photolysis, as previously reported (Berzofsky et al., 1972a).

Oxidation of each isomeric deoxy-sulf-Mb yields spectra clearly corresponding to formation of high-spin ferric products. Since the same met-aquo spectra are produced by oxidation with $Fe(CN)_6^{3-}$ as by autoxidation, the process must involve solely oxidation at the metal center. Reduction of metS_CMbCN with $S_2O_4^{2-}$ produces deoxy-S_CMb; the other isomers are not stable in this reagent.

In the presence of cyanide, each met-aquo isomer exhibits a spectrum indicative of cyanide ligation to the metal center (Berzofsky et al., 1971a; Timkovich & Vavra, 1985; Chatfield et al., 1986a). In the presence of excess hydroxycobalamin, the ligation is reversed, and ^1H NMR spectra are obtained that are identical with those of met-aquo sulf-Mbs observed before CN^- ligation.

The effect of each reagent is reversible for at least one isomer and is obtainable by a separate route for isomers in which it is not reversible. Thus the chemical reagents used to interconvert among the different oxidation/ligation states of individual isomeric sulf-Mbs affect solely the iron center in a manner completely analogous to that of the native protein and do not participate in any alteration of the peripheral functionality of any of the isomers.

Differential Reactivity Patterns of the Isomeric Sulf-Mbs. A key property that interferes with the physiological function of sulfhemoglobin is the decreased ligand affinity (Carrico et al., 1978b). This property is shared by sulf-Mb (Berzofsky et al., 1971b, 1972a). While this reactivity is neither directly addressed nor comprehensively studied in this paper, the above results are strongly suggestive of differential reactivity among the isomeric sulf-Mbs. These differences may be summarized as follows:

(1) The ease with which CO can be removed from carbonyl complexes upon flushing with N_2 or degassing indicates that the affinity for CO of the reduced sulf-Mbs is S_AMb << S_CMb << Mb; data on S_BMb are not available.

(2) It has been reported that the addition of CN^- to a mixture of metS_AMbH_2O and metS_BMbH_2O yields preferential binding to the latter derivative (Chatfield et al., 1986a); in a mixture of metS_AMbH_2O and metS_CMbH_2O preferential binding of CN^- to metS_CMbH_2O is also observed (not shown). Thus, the apparent CN^- affinity is Mb, S_BMb, S_CMb >> S_AMb. The potential origin of this differential activity can be probed by consideration of the removal of CN^- from these proteins. Analysis of parts B and C of Figure 5 shows that, while CN^- is stripped from metMbCN in 1–2 h by hydroxycobalamin, metS_CMbCN remains dominant in the spectrum during this time span. The different rates of CN^- removal must result from differing rates of CN^- dissociation, with Mb possessing a faster off-rate for CN^-. Analogous studies show metS_BMbCN to possess a dissociation rate similar to that of metMbCN, while metS_AMbCN exhibits faster dissociation than the other proteins (not shown).

(3) All deoxy-sulf-Mbs are unstable to the anaerobic addition of $S_2O_4^{2-}$, regenerating native deoxy-Mb; however, deoxy-S_AMb and -S_BMb react with a half-life of seconds, while S_CMb is stable for several hours.[8]

Each isomeric form appears to be distinct in chemical reactivity, with overall ligand affinity and stability toward regeneration of Mb in the order S_CMb > S_BMb > S_AMb. It is likely, therefore, that the oxygen affinities are also different in each isomer, and the need for a careful study of oxygen affinity is indicated.

Structural Properties of Isomeric Sulf-Mbs. The NMR spectra of all of the paramagnetic sulf-Mb derivatives differ from those of the native proteins in the same oxidation/ligation state in that they exhibit considerably reduced symmetry of the prosthetic group, as measured by the spread of the hyperfine-shifted resonances (La Mar, 1979). Such significantly increased rhombic asymmetry strongly suggests disruption of π conjugation to at least one pyrrole. The structure of S_CMb has been established as that depicted in IIc (Chatfield et al., 1986c; Bondoc et al., 1986). The presently available NMR data do not yet provide any new insight into the peripheral functionality for S_AMb or S_BMb, leaving the originally proposed episulfide across the β–β bond, as shown in IIa, as the most reasonable hypothesis for the former species (Berzofsky et al., 1972). The conversion S_AMb → S_CMb thus occurs by insertion of the vinyl C_β to form the thiolene IIc; such a rearrangement is probably determined by protein constraints, which may account for the slow first-order rate. We had proposed that S_BMb represents the ring-opened episulfide (Chatfield et al., 1986c). The acid-catalyzed conversion of S_AMb to S_BMb is consistent with, but not unique for, such ring opening of the episulfide (Gilchrist, 1985). The fact that S_BMb does not convert to S_CMb dictates that the sulfide is attached to C_4 rather than C_3 (structure IIb) if this functionality is correct. Current experiments are directed toward establishing that the same pyrrole is saturated in each of the isomeric sulf-Mbs by identifying the unique unshifted pyrrole methyl in met-aquo complexes using isotope labels (see below). These results will also confirm preliminary data that indicate that sulfglobin formation proceeds only for Mb as defined by

[8] Another reducing agent, sodium ascorbate, also catalyzes regeneration of native proteins from the isomers of sulf-Mb and sulf-Hb, indicating that these agents may have potential clinical relevance to the treatment of sulfhemoglobinemia (Park & Nagel, 1984).

the X-ray crystal structure and not for the form in which the heme is rotated by 90° about the α–γ meso axis (La Mar et al., 1983).

Support for a chlorin-type structure for all three isomeric sulf-Mbs is indirect. The reduced ring current shift for Val-E11 δ-CH_3 in S_AMbCO (A_{10}) and S_CMbCO (C_{10}) (Figure 4) is consistent with saturation of a pyrrole. A very similar decrease in ring current has been reported for the chlorophyll versus magnesium porphyrin complex of sperm whale Mb (Wright & Boxer, 1981). A change in Val-E11 side-chain orientation as the origin of the altered shift, however, cannot be discounted. More direct evidence for decreased ring currents in carbonyl-sulf-Mb complexes can be drawn from the meso-H shifts in the region 8–10 ppm (Figure 4). The differential upfield bias of the likely meso Hs (peaks A_1–A_3 or C_1–C_3) when compared to the native MbCO meso-H shifts (M_1–M_4) is similar to that observed in other chlorins (Scheer & Katz, 1975). Planned assignments of meso Hs by isotope labeling and two-dimensional NMR methods should provide more structural details of the CO complexes of reduced sulf-Mbs.

The presence of only three methyls with significant contact shifts in the three ferric high-spin met-aquo sulf-Mbs (computer-generated spectra for pure species in Figure 6) is further support of a chlorin structure; a fourth methyl must resonate in the crowded diamagnetic envelope. Such a sharp decrease in contact shift for a single pyrrole methyl is reminiscent of other ferric porphyrin derivatives where chemical reaction disrupted π conjugation to a pyrrole, such as with carbene insertion into the Fe–N bond or upon N-alkylation of the porphyrin (Balch et al., 1985a,b). The fact that only one apparent heme methyl exhibits a considerably reduced contact shift supports a model where only a single pyrrole is saturated in each isomer. The known structure of S_CMb (Chatfield et al., 1986b; Bondoc et al., 1986) indicates that its upfield methyl peak in metS_CMbH_2O should arise from the 3-CH_3.

The strong similarities of S_AMb and S_BMb suggested by the proposed structures in IIa and IIb and the distinct differences from S_CMb (IIc) are consistent with the optical spectra, where the former two isomers yield essentially indistinguishable spectra, while for the latter the prominent visible band is consistently red-shifted by 5–18 nm. A similar red-shift has been observed in model chlorins differing only in the presence of the 4-position ethylidene group (Chang & Sotiriou, 1985; Smith et al., 1986). The ^{1}H NMR spectral features for the paramagnetic sulf-Mb derivatives are also more similar between S_AMb and S_BMb than between either of these and S_CMb. Thus, among the met-cyano complexes (Figure 1), only metS_CMbCN exhibits an upfield-shifted 4-H_α (C_{19}) peak and downfield-shifted 4-H_β ($C_{17,18}$) peaks (Chatfield et al., 1986c). Moreover, only metS_CMbH_2O exhibits a strongly upfield-shifted peak (C_{15} in Figure 2G) and two extra downfield peaks, C_{13} and C_{14}, as is also the case for peaks C_8, C_6, and C_7 in deoxy-S_CMb (Figure 3D). Such extremely large π contact shifts in high-spin ferrous hemes are unprecedented [La Mar & Walker (Jensen), 1979]. It is most likely that these unusual shifts also originate from the modified 4-vinyl group, the upfield peaks from the 4-H_α, and the two downfield peaks from the 4-H_βs, as found for metS_CMbCN (Chatfield et al., 1986b).

The unusual ethylidene-type functional group found in S_CMb (IIc) has precedence in bacteriochlorophylls *b* and *g*. Molecular orbital calculations on these complexes indicate that the ethylidene group contributes very strongly to the highest filled π molecular orbital (MO) and negligibly to the lowest vacant π MO (Davis et al., 1979). While similar calculations on chlorins have not yet been reported, the similarity of the π MOs in chlorins and bacteriochlorins (Chang et al., 1981) suggests that a similar situation would apply in chlorins. Thus, the very large π contact shifts indicated by the former 4-vinyl protons demonstrate that the dominant π-bonding interaction involves heme → iron π charge transfer. Somewhat surprising is the observation that such π bonding is stronger in the reduced (deoxy) than in oxidized (met-aquo) S_CMb complexes. However, the stronger π donation in S_CMb is consistent with the greater CO affinity of that isomer (Traylor & Traylor, 1982).

The greatly reduced ligand affinity of sulfglobins relative to that of the native globins has been recognized for some time (Berzofsky et al., 1971b, 1972a; Carrico et al., 1978b; Brittain et al., 1982). Little information exists, however, on the likely origins of this altered reactivity. The present results, moreover, indicate that ligand affinities differ substantially even among the isomeric sulf-Mbs in the order S_AMb < S_BMb < S_CMb < Mb. Ligand affinity in heme proteins is considered to be controlled by proximal axial interactions via the ligated histidyl imidazole, steric perturbations due to distal residue side chains, electronic perturbations through peripheral heme interactions, or any combination of these effects (Traylor & Traylor, 1982). Comparison of the NMR spectral features among sulf-Mb isomers and the native protein in different oxidation/ligation states sheds some light on the likely importance of these various mechanisms.

The labile ring proton of the proximal histidine in high-spin ferrous hemes has been demonstrated to serve as a sensitive indicator of iron–imidazole bonding (La Mar et al., 1977; Nagai et al., 1982). This resonance is observed at 66 ppm in both deoxy-S_AMb and deoxy-S_CMb. While this shift is smaller than for the native protein, it is still within a narrow window of 65–90 ppm where many native deoxy-Mbs and -Hbs that possess normal ligand affinities exhibit this resonance (La Mar, 1979). Moreover, this NH contact shift is identical in S_AMb and S_CMb, even though their CO affinities differ appreciably. Hence we conclude that altered proximal interactions are not primarily responsible for the decreased ligand affinity of sulf-Mbs.

The distal heme pocket can be probed via either the low-spin ferric met-cyano complex or the diamagnetic reduced CO complex of sulf-Mbs. The orientation of the distal His-E7 is clearly detected in the strong downfield shift of its labile ring proton in native metMbCN (Sheard et al., 1970; Cutnell et al., 1981). No such strongly shifted low-field exchangeable proton signals are detected in the met-cyano complexes of any of the isomeric sulf-Mbs (not shown). However, since the His-E7 hyperfine shift is wholly dipolar in origin (Sheard et al., 1970; Cutnell et al., 1981) and it has already been reported that the met-cyano-sulf-Mb complex exhibits significantly reduced magnetic anisotropy (Berzofsky et al., 1971a), a strongly shifted His-E7 signal in met-cyano-sulf-Mb is not expected even if the orientation of this side chain is unaltered upon sulf-Mb formation.

In the diamagnetic carbonyl-sulf-Mb complexes, the reduced Val-E11 δ-CH_3 upfield shift is consistent with the reduced ring current upon chlorin formation without any change in orientation. Moreover, the identical Val-E11 δ-CH_3 shift in both S_AMbCO and S_CMbCO dictates that the distal residue cannot account for the significant differences in CO affinity between these two isomeric sulf-Mbs. Therefore, we conclude that the decreased ligand affinities of sulf-Mbs are very unlikely to be determined primarily by distal steric interactions and hence

that electronic perturbations due to the peripheral modifications must be the determining influence. Moreover, the differential ligand affinities for the three isomeric sulf-Mbs are likely determined by the variable functionality of the saturated pyrrole substituents. At the present time there are no data available on the comparison of CO affinities of iron porphyrins and chlorins possessing an axial nitrogenous base.

Sulfhemoglobin. The ^1H NMR spectrum of met-cyano sulf-Hb in Figure 8 suggests that the two sets of dominant peaks, a, e, f, h, and k and b, g, i, and j, arise from the two nonequivalent subunits reacted to form sulfglobin with structures very similar to S_AMb, as indicated by the characteristic extreme downfield (a and b) and upfield (j and k) methyl peaks when compared with those of S_AMb (A_1 and A_{12}) (Figure 8D). Peaks c and d cannot arise from the same species that yield the two sets of peaks above and hence must represent a second minor product. The absence of other resonances belonging to this set suggests that peaks c and d may be the methyls for the two subunits of the second isomeric sulf-Hb. The single proton peak corresponding to peak c or d would be extremely small and could easily be obscured in the spectrum. The similarity of the shifts of peaks c and d with methyl peak B_1 of metS_BMbCN (Figure 8D) suggests that sulf-Hb may also exhibit two species comparable to S_AMb and S_BMb, with the analogue to the latter present only in <10% components. No resonances could be detected in met-cyano sulf-Hb samples which are analogous to metS_CMbCN, indicating that the thiolene structure (IIc) does not form in sulf-Hb. These preliminary results, however, do indicate that the structural heterogeneity presently characterized for sulf-Mb may have some relevance to sulf-Hb. More detailed studies on sulf-Hb preparation and ^1H NMR spectral characteristics in various oxidation/ligation states are in progress and should permit more quantitative conclusions as to similarities and differences in detailed structures of sulf-Mb and sulf-Hb.

Acknowledgments

We are indebted to A. L. Balch, K. M. Smith, and A. G. Mauk for useful discussions.

References

Andersson, L. A., Loehr, T. M., Lim, A. R., & Mauk, A. G. (1984) *J. Biol. Chem. 259*, 15340–15349.

Antonini, E., & Brunori, M. (1971) *Hemoglobin and Myoglobin in Their Reactions with Ligands*, pp 219–234, North-Holland, Amsterdam.

Balch, A. L., Chan, Y. W., La Mar, G. N., Latos-Grazynski, L., & Renner, M. W. (1985a) *Inorg. Chem. 24*, 1437–1443.

Balch, A. L., Cheng, R. J., La Mar, G. N., & Latos-Grazynski, L. (1985b) *Inorg. Chem. 24*, 2651–2656.

Berzofsky, J. A., Peisach, J., & Blumberg, W. E. (1971a) *J. Biol. Chem. 246*, 3367–3377.

Berzofsky, J. A., Peisach, J., & Blumberg, W. E. (1971b) *J. Biol. Chem. 246*, 7366–7372.

Berzofsky, J. A., Peisach, J., & Alben, J. O. (1972a) *J. Biol. Chem. 247*, 3774–3782.

Berzofsky, J. A., Peisach, J., & Horecker, B. L. (1972b) *J. Biol. Chem. 247*, 3783–3791.

Bondoc, L. L., Chau, M.-H., Price, M. A., & Timkovich, R. (1986) *Biochemistry 25*, 8458–8466.

Bradbury, J. H., Carver, J. A., & Parker, M. W. (1982) *FEBS Lett. 146*, 298–301.

Brittain, T., Greenwood, C., & Barber, D. (1982) *Biochim. Biophys. Acta 705*, 26–32.

Carrico, R. J., Peisach, J., & Alben, J. O. (1978a) *J. Biol. Chem. 253*, 2386–2391.

Carrico, R. J., Blumberg, W. E., & Peisach, J. (1978b) *J. Biol. Chem. 253*, 7212–7215.

Chang, C. K., & Sotiriou, C. (1985) *J. Org. Chem. 50*, 4989–4991.

Chang, C. K., Hanson, L. K., Richardson, P. F., Young, R., & Fajer, J. (1981) *Proc. Natl. Acad. Sci. U.S.A. 78*, 2652–2656.

Chatfield, M. J., La Mar, G. N., Balch, A. L., & Lecomte, J. T. J. (1986a) *Biochem. Biophys. Res. Commun. 135*, 309–315.

Chatfield, M. J., La Mar, G. N., Lecomte, J. T. J., Balch, A. L., Smith, K. M., & Langry, K. C. (1986b) *J. Am. Chem. Soc. 108*, 7108–7110.

Chatfield, M. J., La Mar, G. N., Balch, A. L., Smith, K. M., Parish, D. W., & LePage, T. J. (1986c) *FEBS Lett. 206*, 343–346.

Cutnell, J. D., La Mar, G. N., & Kong, S. B. (1981) *J. Am. Chem. Soc. 103*, 3567–3572.

Davis, M. S., Forman, A., Hanson, L. K., Thornber, J. P., & Fajer, J. (1979) *J. Phys. Chem. 83*, 3325–3332.

De Ropp, J. S., Thanabal, V., & La Mar, G. N. (1985) *J. Am. Chem. Soc. 107*, 8268–8270.

Gilchrist, T. L. (1985) *Heterocyclic Chemistry*, p 111, Pitnam, London.

Hoppe-Seyler, F. (1866) *Zentralbl. Med. Wiss. 4*, 436–438.

Keilin, D. (1933) *Proc. R. Soc. London, B 113*, 394–404.

La Mar, G. N. (1979) in *Biological Applications of Magnetic Resonance* (Shulman, R. G., Ed.) pp 305–343, Academic, New York.

La Mar, G. N., & Walker (Jensen), F. A. (1979) *Porphyrins 4B*, 61–157.

La Mar, G. N., Budd, D. L., & Goff, H. (1977) *Biochem. Biophys. Res. Commun. 77*, 104–110.

La Mar, G. N., Budd, D. L., Sick, H., & Gersonde, K. (1978) *Biochim. Biophys. Acta 537*, 270–283.

La Mar, G. N., Budd, D. L., Smith, K. M., & Langry, K. C. (1980) *J. Am. Chem. Soc. 102*, 1822–1827.

La Mar, G. N., Davis, N. L., Parish, D. W., & Smith, K. M. (1983) *J. Mol. Biol. 168*, 887–896.

Lim, A. R., & Mauk, A. G. (1985) *Biochem. J. 229*, 765–769.

Mabbutt, B. C., & Wright, P. E. (1985) *Biochim. Biophys. Acta 832*, 175–185.

Magliozzo, R. S., & Peisach, J. (1986) *Biochim. Biophys. Acta 872*, 158–162.

Mayer, A., Ogawa, S., Shulman, R. G., Yamana, T., Cavalerio, J. A. S., Rocha-Gonsalves, A. M. d'A, Kenner, G. W., & Smith, K. M. (1974) *J. Mol. Biol. 86*, 749–756.

Morell, D. B., Chang, Y., & Clezy, P. S. (1967) *Biochim. Biophys. Acta 13*, 121–130.

Nagai, K., Hori, H., Morimoto, H., Hayashi, A., & Taketa, F. (1979) *Biochemistry 18*, 1304–1308.

Nagai, K., La Mar, G. N., Jue, T., & Bunn, H. F. (1982) *Biochemistry 21*, 842–847.

Nicholls, P. (1961) *Biochem. J. 81*, 374–383.

Ogawa, S., Shulman, R. G., Fujiwara, M., & Yamane, T. (1972) *J. Mol. Biol. 70*, 301–313.

Park, C. M., & Nagel, R. L. (1984) *N. Engl. J. Med. 310*, 1579–1584.

Pratt, J. M. (1982) in B_{12} (Dolphin, D., Ed.) p 337, Wiley, New York.

Scheer, H. S., & Katz, J. J. (1975) in *Porphyrins and Metalloporphyrins* (Smith, K. S., Ed.) pp 339–524, Elsevier, New York.
Sheard, B., Yamane, T., & Shulman, R. G. (1970) *J. Mol. Biol. 53*, 25–48.
Shulman, R. G., Wüthrich, K., Yamane, T., Antonini, E., & Brunori, M. (1969) *Proc. Natl. Acad. Sci. U.S.A. 63*, 623–628.
Smith, K. M., Simpson, D. J., & Snow, K. M. (1986) *J. Am. Chem. Soc. 108*, 6834–6835.
Timkovich, R., & Vavra, M. R. (1985) *Biochemistry 24*, 5189–5196.
Traylor, T. G., & Traylor, P. S. (1982) *Annu. Rev. Biophys. Bioeng. 11*, 105–127.
Wright, K. A., & Boxer, S. G. (1981) *Biochemistry 20*, 7546–7556.

Prediction of a Common Structural Domain in Aminoacyl-tRNA Synthetases through Use of a New Pattern-Directed Inference System†

Teresa A. Webster,* Richard H. Lathrop, and Temple F. Smith

Molecular Biology Computer Research Resource, Dana-Farber Cancer Institute, Harvard School of Public Health, Boston, Massachusetts 02115, and Artificial Intelligence Laboratory, Massachusetts Institute of Technology, Cambridge, Massachusetts 02139

Received January 7, 1987; Revised Manuscript Received May 13, 1987

ABSTRACT: The aminoacyl-tRNA synthetases are united by a common function with little evidence of a common structural relationship. Outside of an 11 amino acid stretch called the "signature sequence", no global primary sequence similarity exists. The signature sequence matches 4–11 amino acids in several aminoacyl-tRNA synthetases. High-resolution X-ray data are available for two of these enzymes, revealing that their signature sequence regions are small segments of a common mononucleotide binding foldlike structure. A new methodology for the analysis of dissimilar primary sequences supports the expectation that all of the signature sequence regions form a common structure. In our analysis, two complex pattern descriptors were constructed to describe the synthetase mononucleotide binding fold. These were compared to primary sequences annotated with predicted secondary structures and hydropathy profiles. Regions in 8 out of 12 (67%) heterologous aminoacyl-tRNA synthetase groups (where each group is specific for the same amino acid) match the first descriptor, and 7 of these (58%) also match the second descriptor. In contrast, only 4 regions in a set of 54 control proteins (7.4%) match the first descriptor, and only 2 regions (3.7%) match both. Alignment of these 8 regions to the descriptor (1) positions all known signature sequence regions as the first loop of a mononucleotide binding foldlike structure, (2) extends the previous alignments by another 40-odd amino acids, and (3) identifies potential sites in 3 out of 6 heterologous aminoacyl-tRNA synthetases with no previous alignments. Potential sites are also proposed for two additional heterologous synthetases on the basis of matches to less specific descriptors.

Aminoacyl-tRNA synthetases share a common function, which is to attach an amino acid to its cognate tRNA in protein biosynthesis. Despite this, they have little to unite them as common protein structures (Schimmel & Söll, 1979; Schimmel, 1987). Their quaternary structures vary from α, α_2, and α_4 to $\alpha_2\beta_2$, and the individual subunits, which contain a complete set of substrate sites, range in size from 300 to 1000 amino acids. Twenty-two aminoacyl-tRNA synthetase sequences have been generated from three bacterial species and from *Saccharomyces cerevisiae* [reviewed by Schimmel (1987)]. These form 12 heterologous groups of synthetases, each specific for the same amino acid. Throughout this paper, synthetases in the same group are usually referred to as one type of 12 heterologous synthetases. Synthetases within the same group share primary sequence similarities of high statistical significance and are therefore believed to be homologous. However, computer searches for sequence similarities between pairs of synthetases from different groups have not revealed any extended regions of similarity (Hountondji et al., 1986a,b; Schimmel, 1987).

Four lines of evidence suggest that common structures may exist among heterologous synthetases. One, high-resolution X-ray structures are available for *Bacillus stearothermophilus* Tyr-tRNA synthetase and a fragment of *Escherichia coli* Met-tRNA synthetase. These reveal the existence of a common structure found in many nucleotide binding proteins: the Rossman mononucleotide binding fold (MNBF) (Rossman et al., 1975; Zewler et al., 1982; Blow et al., 1983). From co-crystal structures of the nucleotide-bound enzymes and from site-specific mutagenesis studies, the function of this domain is implied to be the binding of ATP and the aminoacyl adenylate [reviewed by Blow and Brick (1985)]. Two, the Ile-, Glu-, Gln-, and Trp-tRNA synthetases, whose structures are unknown, all contain "signature sequence" regions (Figure 1) which match sequences within the Tyr- and Met-tRNA synthetase MNBF-like structures (Barker & Winter, 1982; Webster et al., 1984; Myers & Tzagoloff, 1985; Breton et al.,

† This work was supported in part by NIH Grant RR02275 and by DARPA under ONR Contract N0014-80-C-0505.
* Address correspondence to this author at the Molecular Biology Computer Research Resource, Dana-Farber Cancer Institute.

0006-2960/87/0426-6950$01.50/0